Spectral resolved Measurement of the Nitrogen Fluorescence Emissions in Air induced by Electrons

T. Waldenmaier[1], J. Blümer[2,3], H. Klages[2]

[1]Bartol Research Institute,

[2]Forschungszentrum Karlsruhe,

[3]Universität Karlsruhe

Aspen Workshop on Cosmic Ray Physics, April 16, 2007

Outline

Motivation

Questions to answer

- Temperature-, pressure-dependence ?
- Energy dependence ?
- Absolute value of $Y(\lambda, p, T)$?

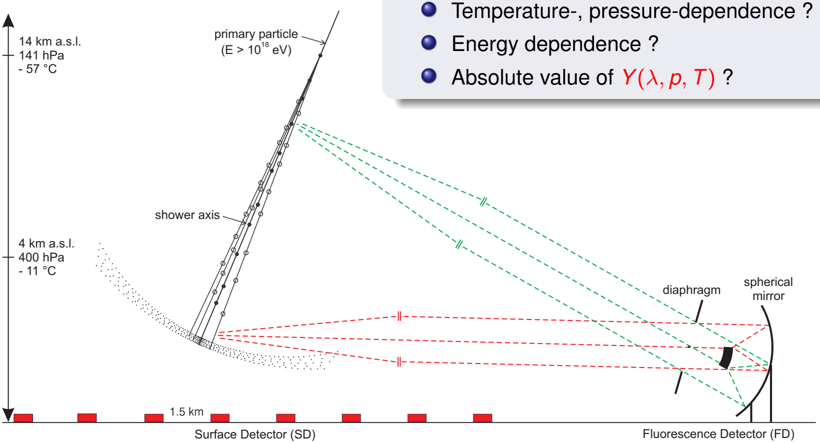

$$\frac{dN_\gamma^{obs}}{dX} = \frac{dE_{dep}}{dX} \cdot \int Y(\lambda, p, T) \cdot T_{atm}(\lambda) \cdot \varepsilon_{det}(\lambda)\, d\lambda$$

Nitrogen Fluorescence Spectrum

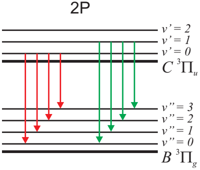

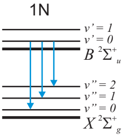

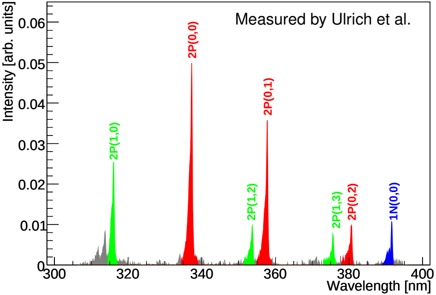

Properties

- Rotational-vibrational spectrum.
- Mainly three electronic-vibrational band systems between 300 nm and 400 nm: $2P(v' = 0, v'')$, $2P(v' = 1, v'')$, $1N(v' = 0, v'')$
- Intrinsic (radiative) transition rate: $\frac{1}{\tau_{0\,v'}} = \sum_{v''} \frac{1}{\tau_{v' \to v''}}$
- Constant intensity ratios between transitions within a vibrational band system.

Collisional Quenching

Additional radiationless deactivations via collisional energy transfer

- Total transition rate: $\frac{1}{\tau_{v'}} = \frac{1}{\tau_{0\,v'}} + \frac{1}{\tau_{c\,v'}}$
- Collisional quenching rate: $\frac{1}{\tau_{c\,v'}} = \sum_x Q^x_{v'}(T) \cdot n_x \quad , x = N_2, O_2, Ar, H_2O, \ldots$
- Quenching rate "constant": $Q^x_{v'}(T) \propto \sqrt{T}$ $(\rightarrow$ kinetic gas theory)
- Number density: $n_x = \frac{p_x}{kT} = \frac{f_x}{kT} \cdot p$

$$\Downarrow$$

Total transition rate

$$\frac{1}{\tau_{v'}} = \frac{1}{\tau_{0\,v'}} \cdot \left(1 + p \cdot \underbrace{\frac{\tau_{0\,v'}}{kT} \sum_x f_x \cdot Q^x_{v'}(T)}_{1/p'_{v'}(T)}\right) = \frac{1}{\tau_{0\,v'}} \cdot \left(1 + \frac{p}{p'_{v'}(T)}\right)$$

$\rightarrow$ linear pressure-dependence for constant mixing ratios and temperatures.

Fluorescence Yield

Fluorescence yield for any transition from same electronic-vibrational level v':

$$Y_{v',v''}(E,p,T) = Y^0_{v'}(E) \cdot R_{v',v''} \cdot \frac{\tau_{v'}(p,T)}{\tau_{0\,v'}} \qquad \left[\frac{photons}{dep.\ energy}\right]$$

Ingredients

- Intrinsic fluorescence yield of most intensive transition: $Y^0_{v'}(E)$ $\left[\frac{photons}{dep.\ energy}\right]$
- Constant intensity ratios $R_{v',v''}$ relative to most intensive transition.
- Fraction of radiative transitions: $\frac{\tau_{v'}(p,T)}{\tau_{0\,v'}} = \frac{radiative\ rate}{total\ rate}$

Fluorescence Yield

Fluorescence yield for any transition from same electronic-vibrational level v':

$$Y_{v',v''}(E,p,T) = Y^0_{v'}(E) \cdot R_{v',v''} \cdot \frac{\tau_{v'}(p,T)}{\tau_{0\,v'}} \qquad \left[\frac{photons}{dep.\ energy}\right]$$

Ingredients

- Intrinsic fluorescence yield of most intensive transition: $Y^0_{v'}(E)$ $\left[\frac{photons}{dep.\ energy}\right]$
- Constant intensity ratios $R_{v',v''}$ relative to most intensive transition.
- Fraction of radiative transitions: $\frac{\tau_{v'}(p,T)}{\tau_{0\,v'}} = \frac{radiative\ rate}{total\ rate}$

Fluorescence Yield

Fluorescence yield for any transition from same electronic-vibrational level v':

$$Y_{v',v''}(E,p,T) = Y^0_{v'}(E) \cdot R_{v',v''} \cdot \frac{\tau_{v'}(p,T)}{\tau_{0\,v'}} \qquad \left[\frac{photons}{dep.\ energy}\right]$$

Ingredients

- Intrinsic fluorescence yield of most intensive transition: $Y^0_{v'}(E)$ $\left[\frac{photons}{dep.\ energy}\right]$
- Constant intensity ratios $R_{v',v''}$ relative to most intensive transition.
- Fraction of radiative transitions: $\frac{\tau_{v'}(p,T)}{\tau_{0\,v'}} = \frac{radiative\ rate}{total\ rate}$

Fluorescence Yield

Fluorescence yield for any transition from same electronic-vibrational level v':

$$Y_{v',v''}(E,p,T) = Y^0_{v'}(E) \cdot R_{v',v''} \cdot \frac{\tau_{v'}(p,T)}{\tau_{0\,v'}} \qquad \left[\frac{photons}{dep.\ energy}\right]$$

Ingredients

- Intrinsic fluorescence yield of most intensive transition: $Y^0_{v'}(E)$ $\left[\frac{photons}{dep.\ energy}\right]$
- Constant intensity ratios $R_{v',v''}$ relative to most intensive transition.
- Fraction of radiative transitions: $\frac{\tau_{v'}(p,T)}{\tau_{0\,v'}} = \frac{radiative\ rate}{total\ rate}$

Fluorescence Yield

Fluorescence yield for any transition from same electronic-vibrational level v':

$$Y_{v',v''}(E,p,T) = Y^0_{v'}(E) \cdot R_{v',v''} \cdot \frac{\tau_{v'}(p,T)}{\tau_{0\,v'}} \qquad \left[\frac{photons}{dep.\ energy}\right]$$

Ingredients

- Intrinsic fluorescence yield of most intensive transition: $Y^0_{v'}(E)$ $\left[\frac{photons}{dep.\ energy}\right]$
- Constant intensity ratios $R_{v',v''}$ relative to most intensive transition.
- Fraction of radiative transitions: $\frac{\tau_{v'}(p,T)}{\tau_{0\,v'}} = \frac{radiative\ rate}{total\ rate}$

Advantages of this representation

- Consistent description.
- Separation of excitation and de-excitation processes.
- Does not depend on energy loss function (Bethe-Bloch or similar).
- Clear meaning of parameters.

Fluorescence Yield

Fluorescence yield for any transition from same electronic-vibrational level v':

$$Y_{v',v''}(E,p,T) = Y^0_{v'}(E) \cdot R_{v',v''} \cdot \frac{\tau_{v'}(p,T)}{\tau_{0\,v'}} \qquad \left[\frac{photons}{dep.\ energy}\right]$$

Ingredients

- Intrinsic fluorescence yield of most intensive transition: $Y^0_{v'}(E)$ $\left[\frac{photons}{dep.\ energy}\right]$
- Constant intensity ratios $R_{v',v''}$ relative to most intensive transition.
- Fraction of radiative transitions: $\frac{\tau_{v'}(p,T)}{\tau_{0\,v'}} = \frac{radiative\ rate}{total\ rate}$

$\Rightarrow$ All these parameters have been measured with the AirLight-Experiment ...

Setup of the AirLight Experiment

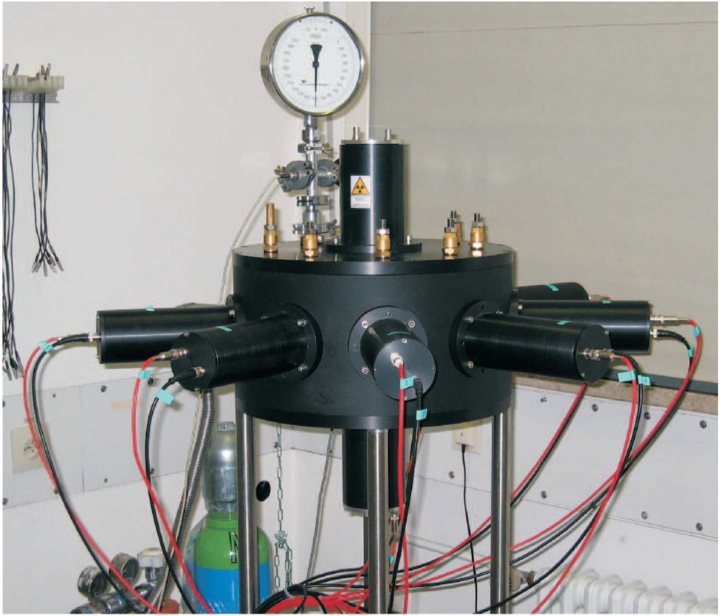

Setup of the AirLight Experiment

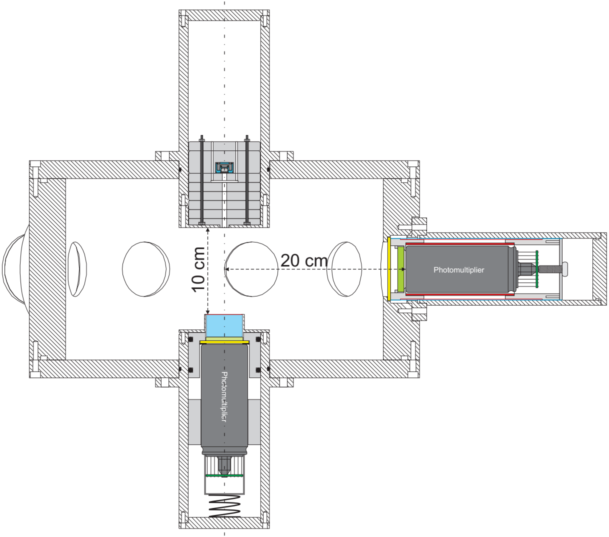

Setup of the AirLight Experiment

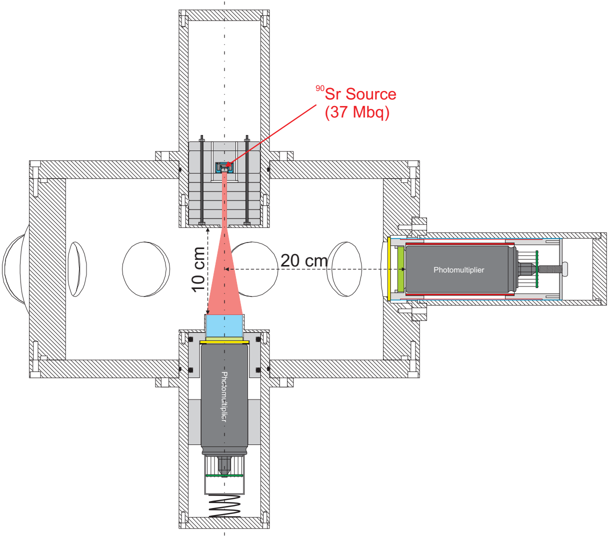

Setup of the AirLight Experiment

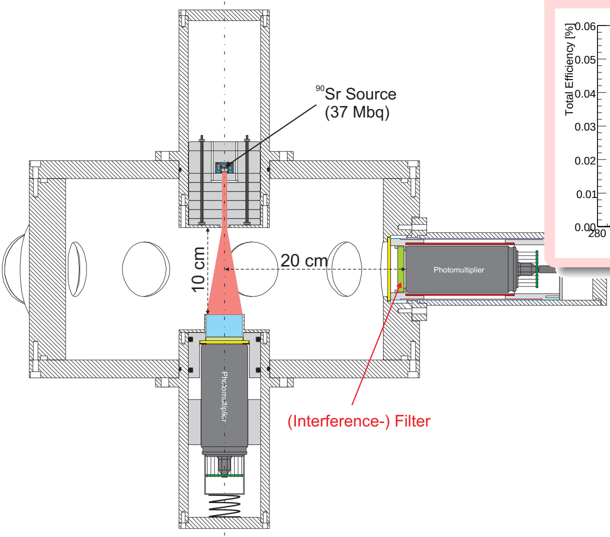

Filter Efficiencies

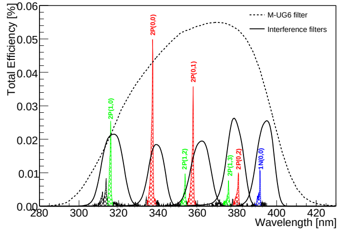

Setup of the AirLight Experiment

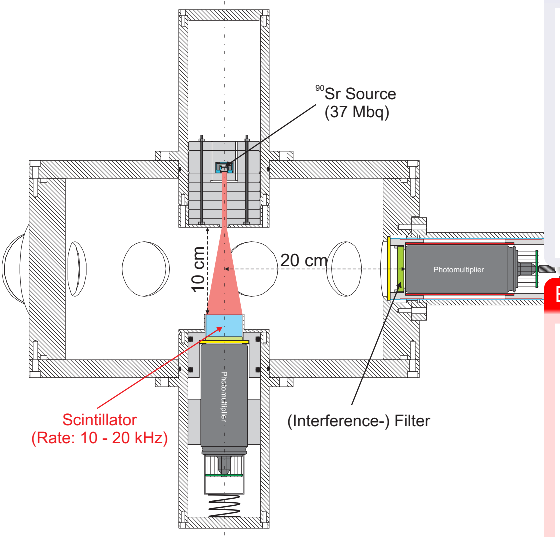

Filter Efficiencies

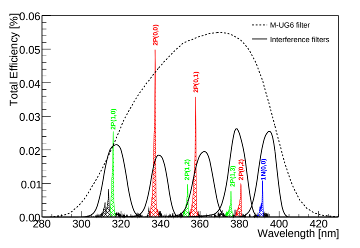

Energy Spectra @ Scintillator

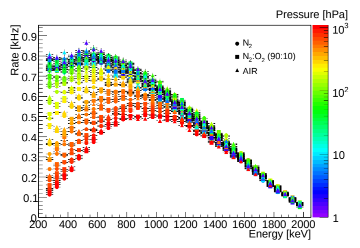

Data Acquisition

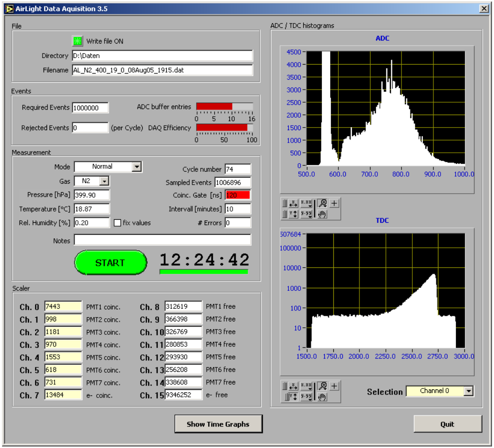

Measurement of coincidences between electron- and photon-detectors:

- Pulse height distributions.
- Difference-time spectra.
- Absolute scaler values.
- Coincident/free electron energy spectra.

Additional monitoring of:

- Pressure.
- Temperature.
- Relative Humidity.
- Free/Coincident event rates.
- High Voltage/Current.

Data Acquisition

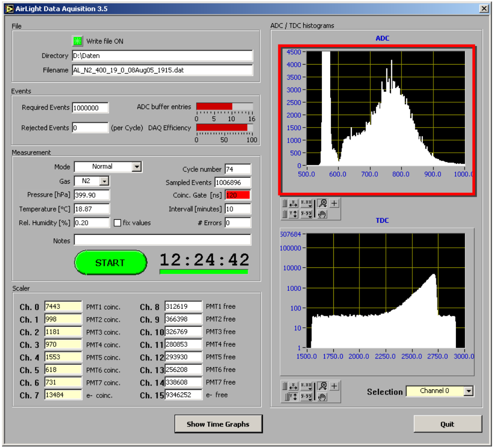

Measurement of coincidences between electron- and photon-detectors:

- Pulse height distributions.
- Difference-time spectra.
- Absolute scaler values.
- Coincident/free electron energy spectra.

Additional monitoring of:

- Pressure.
- Temperature.
- Relative Humidity.
- Free/Coincident event rates.
- High Voltage/Current.

Data Acquisition

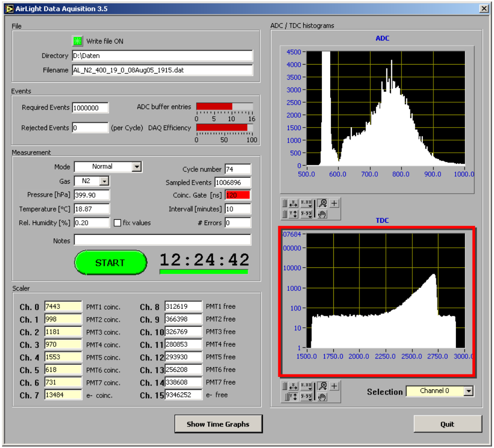

Measurement of coincidences between electron- and photon-detectors:

- Pulse height distributions.
- Difference-time spectra.
- Absolute scaler values.
- Coincident/free electron energy spectra.

Additional monitoring of:

- Pressure.
- Temperature.
- Relative Humidity.
- Free/Coincident event rates.
- High Voltage/Current.

Data Acquisition

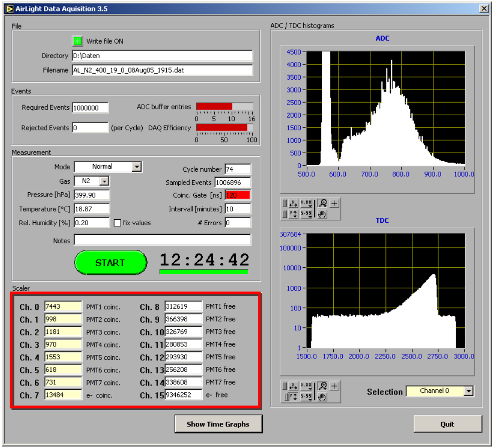

Measurement of coincidences between electron- and photon-detectors:

- Pulse height distributions.
- Difference-time spectra.
- Absolute scaler values.
- Coincident/free electron energy spectra.

Additional monitoring of:

- Pressure.
- Temperature.
- Relative Humidity.
- Free/Coincident event rates.
- High Voltage/Current.

Data Acquisition

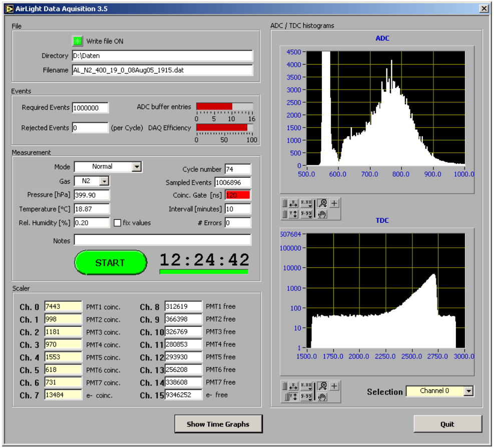

Measurement of coincidences between electron- and photon-detectors:

- Pulse height distributions.
- Difference-time spectra.
- Absolute scaler values.
- Coincident/free electron energy spectra.

Additional monitoring of:

- Pressure.
- Temperature.
- Relative Humidity.
- Free/Coincident event rates.
- High Voltage/Current.

GEANT4 Simulation (version 7.1)

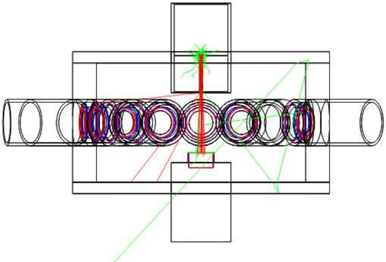

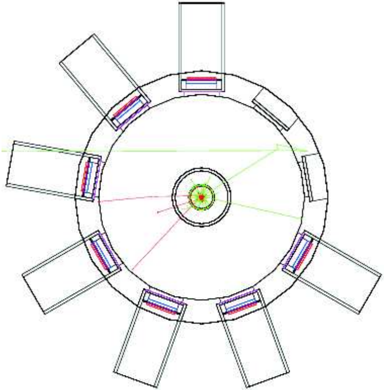

- Electron energy spectra.
- Energy deposit in chamber.
- Photon angle distribution and acceptance of photomultipliers.

^{90}Sr Energy Spectrum

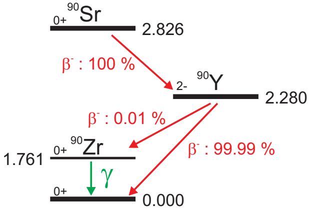

$$^{90}_{38}\mathrm{Sr} \xrightarrow{t_{1/2}\,=\,29\ \mathrm{a}} {}^{90}_{39}\mathrm{Y} \xrightarrow{t_{1/2}\,=\,64\ \mathrm{h}} {}^{90}_{40}\mathrm{Zr}$$

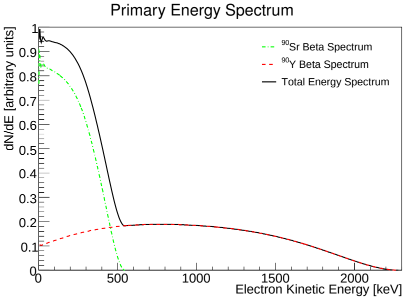

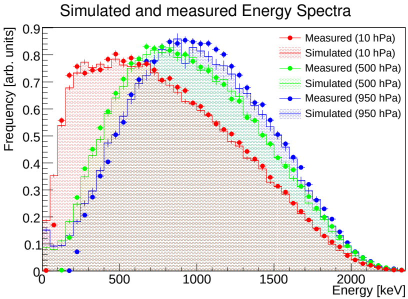

- Distorted spectral shape due to backscattering in the collimator.
- Pressure dependence due to multiple scattering and energy losses in the gas.
- Good overall agreement of simulated and measured spectra.

Energy deposit in chamber

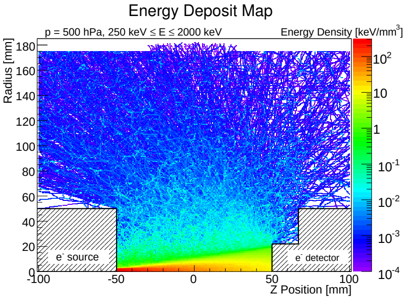

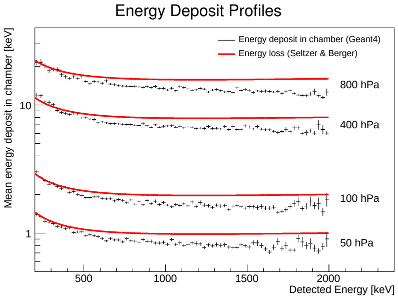

- $\langle E_{dep} \rangle$ about 15 % to 20 % smaller than $\langle E_{loss} \rangle$ due to limited chamber volume.
- Influence of delta electrons is correctly treated.
- Energy Deposit Maps generated for all pressures used for the measurements.

Angle Distribution & Acceptance

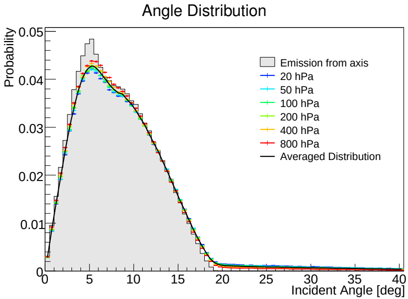

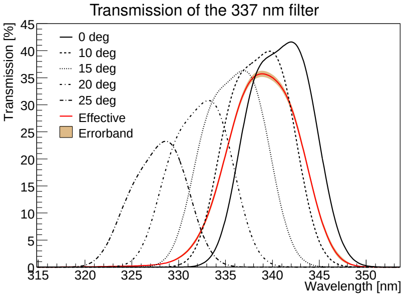

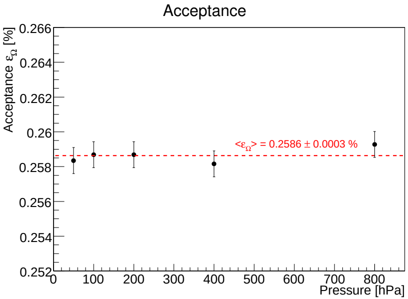

- Assumption: $\#Photons \propto E_{dep}$.

$\rightarrow$ Generation of optical photons according to energy deposit maps.

- Slight pressure dependence of angular distributions ($\rightarrow$ averaging).

- Acceptance $\varepsilon_\Omega = \frac{\#detected\ photons}{\#generated\ photons}$

Energy Calibration

Calibration with ^{22}Na-Source

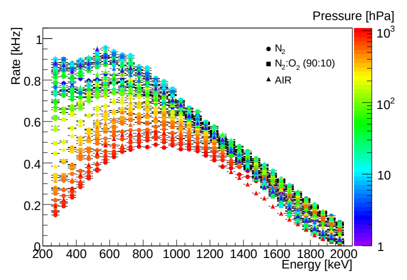

- Special calibration runs.
- Calibration with ^{22}Na-Compton-Spectrum (Compton edges at 341 keV and 1062 keV).
- Smearing with Gaussian resolution function.

Calibration with MC Spectra

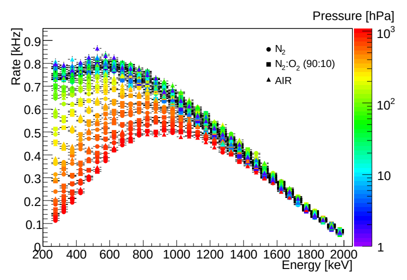

- Individual calibration of each run.
- Calibration with simulated ^{90}Sr-spectra (Covers the whole energy range).
- Smearing with Gaussian resolution function.

- Both methods result in an energy resolution of $\frac{\sigma_E}{E} \approx 10\% \cdot \sqrt{\frac{1\,MeV}{E}}$.
- MC-calibration yields consistent spectra and minimizes run-to-run fluctuations.
- Using MC-calibration!

Relative Calibration of the Photomultipliers

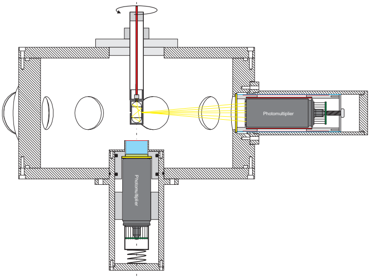

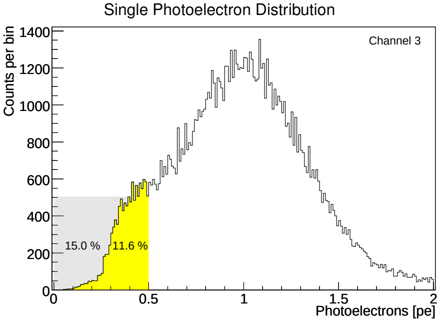

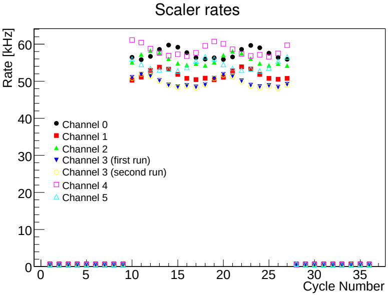

- Detected photons: $N_{det} = \varepsilon_\Omega \cdot \varepsilon_s \cdot f_{cal} \cdot N_0$
- $\varepsilon_s = \int_\lambda \varepsilon^0_{QE}(\lambda) \cdot T(\lambda) \cdot \frac{dN}{d\lambda}\, d\lambda = const.$
- Photoelectron cut: $0.5 \leq p.e. \leq 2.0$ (for calibration and measurement)
- Calibration relative to channel 3 ($f_{cal} \equiv 1$)
- Monthly fluctuations of $f_{cal} \lesssim 3\%$.

Absolute Uncertainties

Relative Uncertainty

Relative calibration f_{cal}:	~ 3 %
Photoelectron cut ε_{cut}:	~ 2 %
Spectral efficiency ε_s:	$4 - 8$ %
Acceptance ε_Ω:	~ 0.4 %
Total:	$5.4 - 8.8$ %

Detection efficiency: $\varepsilon_{det} = \varepsilon_\Omega \cdot \varepsilon_s \cdot f_{cal} \cdot f_{cal}^3$

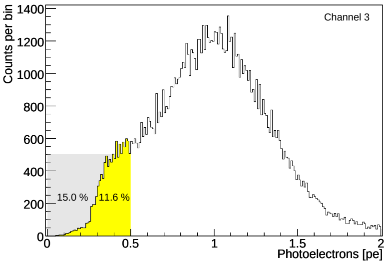

Absolute estimation of f_{cal}^3:

- About 12 % of the events are between discr. threshold and 0.5 pe.
- Roughly (7.5 ± 7.5) % of the events are below discr. threshold.
- Normalization error of QE-curve assumed to be $\sim$ 10%.

$$\Rightarrow \quad f_{cal}^3 = \underbrace{(1 \pm 10\,\%)}_{QE\ norm.} \cdot \underbrace{(1 + 12\,\% + 7.5\,\% \pm 7.5\,\%)^{-1}}_{\varepsilon_{cut}} = 0.837 \pm 0.099 \quad (\Delta f_{cal}^3 = 12\,\%)$$

$\Rightarrow$ Absolute accuracy of detection efficiencies of single bands: $\lesssim 15$ %

Measurements & Data Analysis

Dataset used for the analysis consists of $\sim$ 50 runs with:

- Pure nitrogen
- Dry air (78% N_2, 21% O_2, 1% Ar)
- Mixture (90% N_2, 10% O_2)
- Nitrogen + water vapor
- Temperature: $\sim$ 20°C
- Pressure range: 2 hPa - 990 hPa
- Energy range: 250 keV - 2000 keV
- Duration: 12 h - 30 h (depending on gas and pressure)

"Step one: take a good stiff drink."

Analysis philosophy:

Step 1: Determination of quenching parameters and intensity ratios over whole energy range ($\rightarrow$ max. statistics).

Step 2: Determination of intensities (intrinsic yields) with fixed parameters of Step 1 for energy sub-ranges.

Fitting Procedure

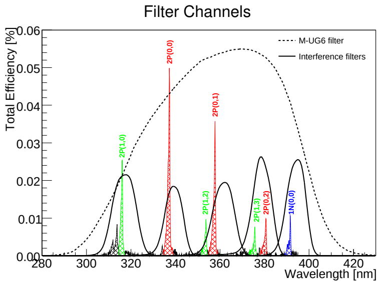

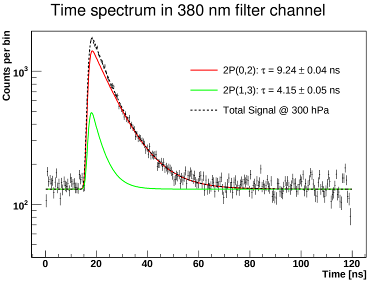

Time distribution in a single filter channel:

$$\frac{dN}{dt} = \frac{1}{2} \cdot \sum_{v'} \sum_{v''} \frac{\varepsilon_{det}^{v',v''} \cdot R_{v',v''} \cdot N_{v'}^{0}}{\tau_{v'}} \cdot e^{-\frac{t-t_0}{\tau_{v'}}} \cdot e^{\frac{\sigma_t^2}{2\tau_{v'}^2}} \cdot \mathrm{erfc}\left(\frac{t_0 - t - \frac{\sigma_t^2}{\tau_{v'}}}{\sqrt{2}\sigma_t} \right)$$

$N_{v'}^{0}$: Absolute number of photons emitted by main transition of state v'.

$\tau_{v'}$: Common lifetime for all transitions $v' \longrightarrow v''$.

$R_{v',v''}$: Intensity ratio with respect to main transition (same for all measurements).

$\Rightarrow$ Simultaneous fit of all filter channels and all runs to determine $N_{v'}^{0}$, $\tau_{v'}$, $R_{v',v''}$.

Time Spectra in Nitrogen at 20 hPa

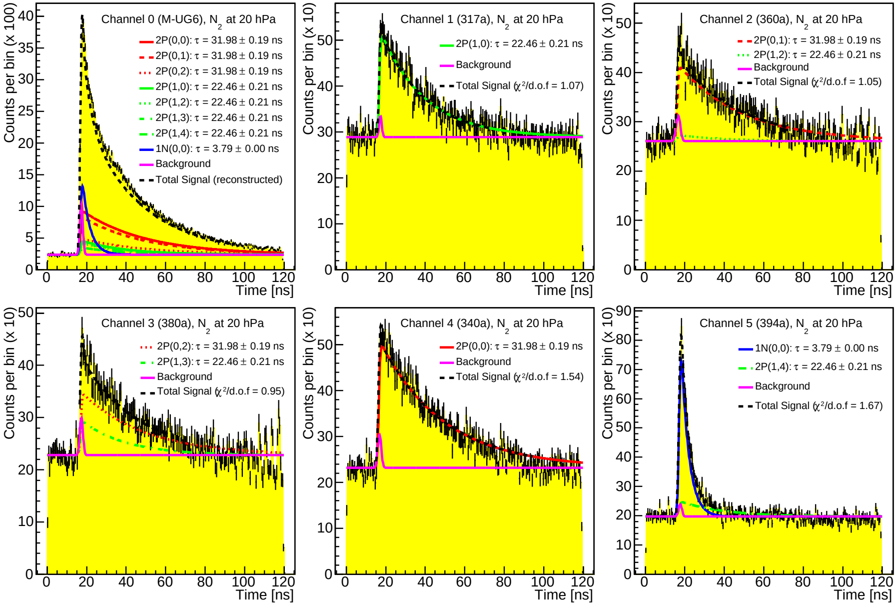

Time Spectra in Nitrogen at 100 hPa

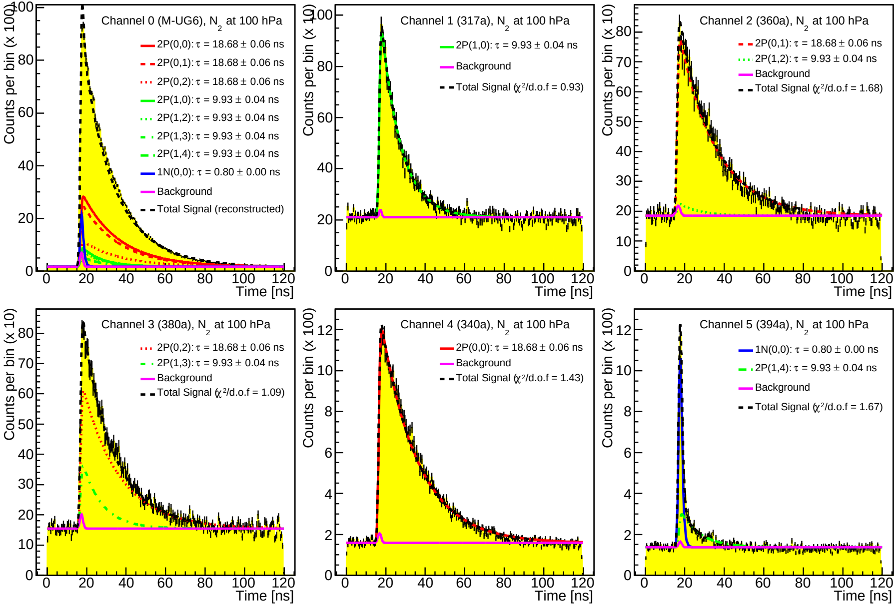

Time Spectra in Nitrogen at 800 hPa

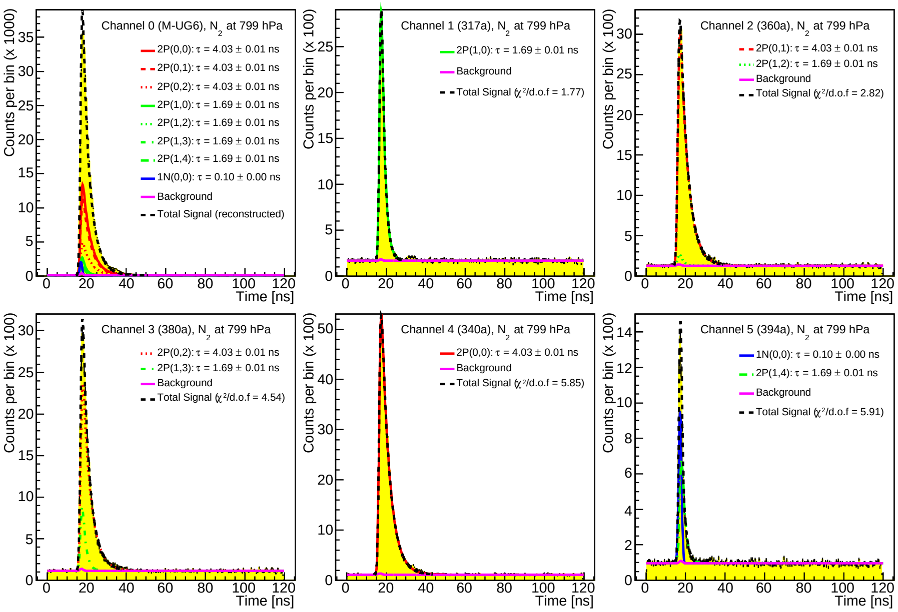

Reconstructed Signal in M-UG6 channel:

M-UG6 Signal

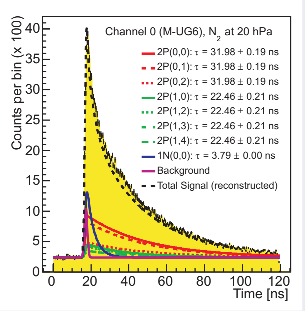

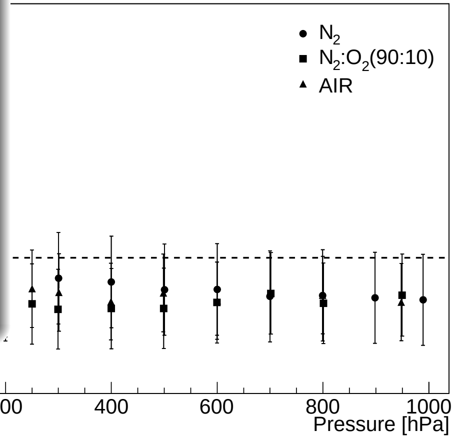

- Good description of the total fluorescence yield over whole pressure range.
- Contributions of neglected nitrogen transitions are less than 4 %.

Reconstructed Signal in M-UG6 channel:

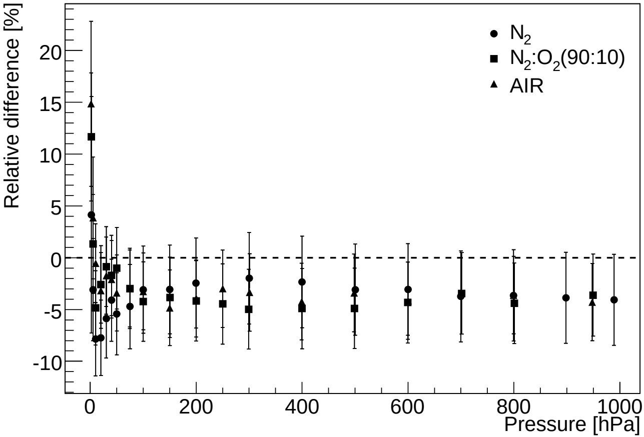

- Good description of the total fluorescence yield over whole pressure range.
- Contributions of neglected nitrogen transitions are less than 4 %.

Nitrogen Quenching Results

2P(0,v”)

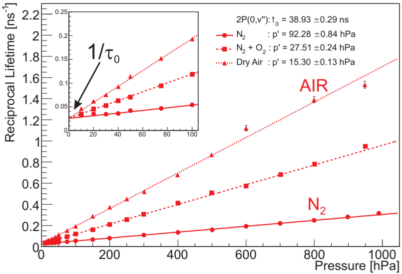

2P(1,v”)

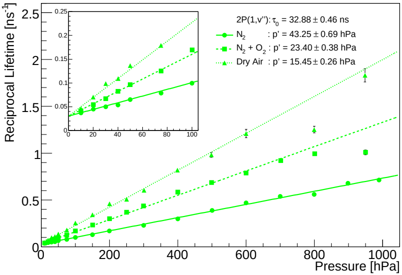

1N(0,0)

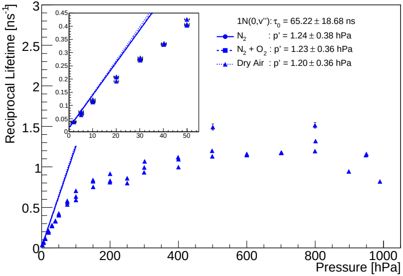

Additional constraint:

$$\frac{1}{\tau_{v'}} = \frac{1}{\tau_{0\,v'}} \cdot \left(1 + p \cdot \underbrace{\frac{\tau_{0\,v'}}{kT} \sum_x f_x \cdot Q^x_{v'}(T)}_{1/p'(T)}\right)$$

- Results represented by lines.
- Better separation of 1N(0,0) band.

Nitrogen Quenching Results

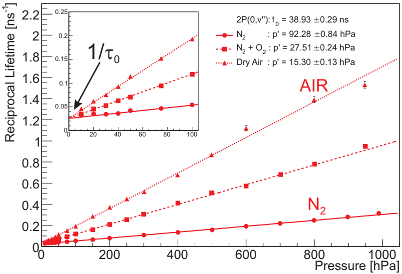

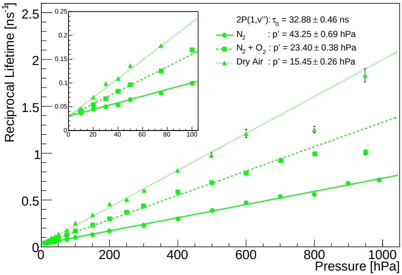

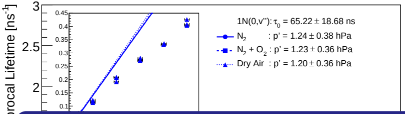

Additional constraint:

$$\frac{1}{\tau_{v'}} = \frac{1}{\tau_{0\,v'}} \cdot \left(1 + p \cdot \frac{\tau_{0\,v'}}{kT} \sum_x f_x \cdot Q^x_{v'}(T)\right)$$

Fitting function

$$\frac{dN}{dt} = \frac{1}{2} \cdot \sum_{v'} \sum_{v''} \frac{\varepsilon_{det}^{v',v''} \cdot R_{v',v''} \cdot N^0_{v'}}{\tau_{v'}} \cdot e^{-\frac{t-t_0}{\tau_{v'}}} \cdot e^{\frac{\sigma_t^2}{2\tau_{v'}^2}} \cdot \mathrm{erfc}\left(\frac{t_0 - t - \frac{\sigma_t^2}{\tau_{v'}}}{\sqrt{2}\sigma_t}\right)$$

Nitrogen Quenching Results

2P(0,v")

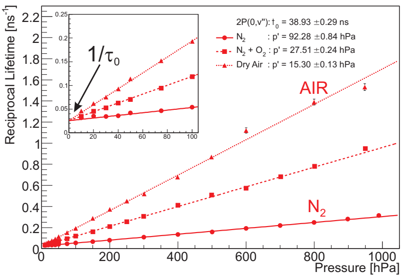

2P(1,v")

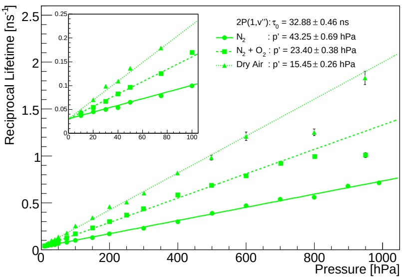

1N(0,0)

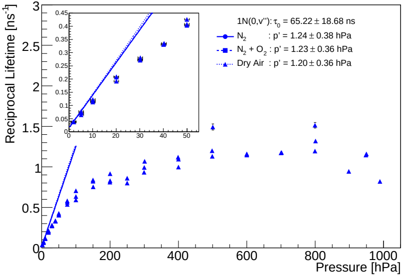

Additional constraint:

$$\frac{1}{\tau_{v'}} = \frac{1}{\tau_{0\,v'}} \cdot \left(1 + p \cdot \underbrace{\frac{\tau_{0\,v'}}{kT} \sum_{x} f_x \cdot Q^x_{v'}(T)}_{1/p'(T)}\right)$$

- Results represented by lines.
- Better separation of 1N(0,0) band.

Nitrogen Quenching Results

2P(0,v")

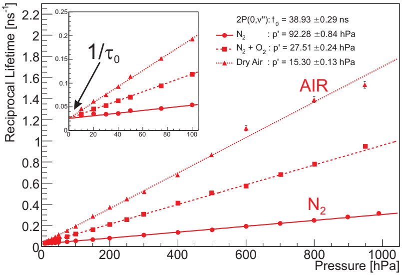

2P(1,v")

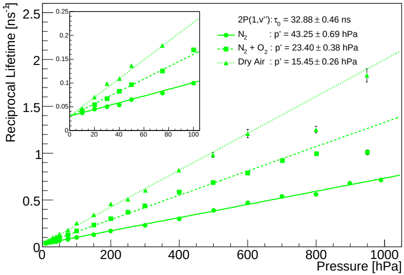

1N(0,0)

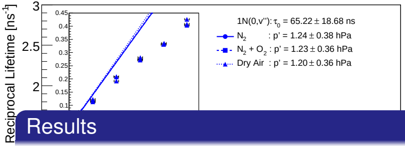

Additional constraint:

$$\frac{1}{\tau_{v'}} = \frac{1}{\tau_{0\,v'}} \cdot \left(1 + p \cdot \frac{\tau_{0\,v'}}{kT} \sum_x f_x \cdot Q^x_{v'}(T)\right)$$

Results

		2P(0,v")	2P(1,v")	1N(0,v")
τ_0	[ns]	38.9 ± 0.30	32.9 ± 0.50	65.2 ± 18.7
Q_{N_2}	[$10^{-10} cm^3 s^{-1}$]	0.11 ± 0.00	0.29 ± 0.00	5.00 ± 0.17
Q_{O_2}	[$10^{-10} cm^3 s^{-1}$]	2.76 ± 0.01	2.70 ± 0.03	5.24 ± 0.79

The Effect of Water Vapor

Measurements with pure nitrogen at 30 hPa plus a variable amount of water vapor:

2P(0,v”) and 2P(1,v”)

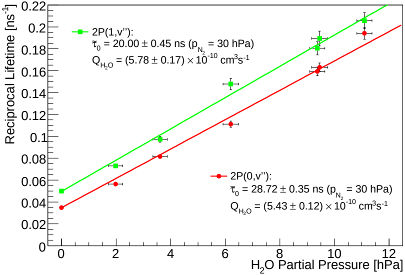

1N(0,v”)

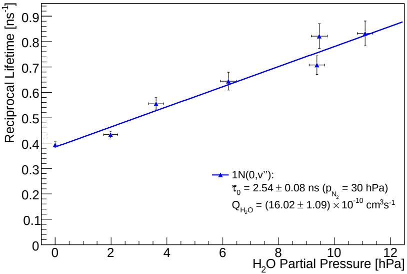

Results

	Q_{H_2O} $[10^{-10} cm^3 s^{-1}]$
2P(0,v”)	5.43 ± 0.12
2P(1,v”)	5.78 ± 0.17
1N(0,v”)	16.02 ± 1.09

Large quenching rate constant of 1N system due to polar nature of ionized nitrogen!?

Step 2: Energy dependence of Intrinsic Yield

Determination of intrinsic yield in sub-samples of 250 keV energy bins:

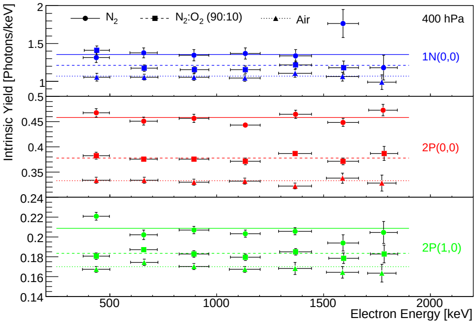

Fluorescence Yield:

$$Y^0_{v'}(E) \cdot R_{v',v''} \cdot \frac{\tau_{v'}(p,T)}{\tau_{0\,v'}} = \frac{N_\gamma(E,p,T)}{N_e \cdot \langle E_{dep}(E,p,T)\rangle}$$

- $R_{v',v''}$, $\tau_{v'}(p,T)$ and $\tau_{0\,v'}$ known from Step 1.
- Deposited energy $\langle E_{dep}(E,p,T)\rangle$ determined by GEANT4 simulation.
- Number of emitted photons $N_\gamma(E,p,T)$ obtained from fit.

$\Rightarrow$ No energy dependence of $Y^0_{v'}(E)$ in investigated range. $\Leftrightarrow$ $N_\gamma \propto E_{dep}$

Intrinsic Yields of dry air in [Photons/keV]

	2P(0,0)	2P(1,0)	1N(0,0)
This work	$0.338 \pm 0.001 \pm 0.051$	$0.172 \pm 0.001 \pm 0.025$	$1.048 \pm 0.007 \pm 0.154$
Nagano et al.	$0.272 \pm 0.007 \pm 0.035$	$0.122 \pm 0.007 \pm 0.016$	$0.303 \pm 0.012 \pm 0.039$

Step 2: Energy dependence of Intrinsic Yield

Determination of intrinsic yield in sub-samples of 250 keV energy bins:

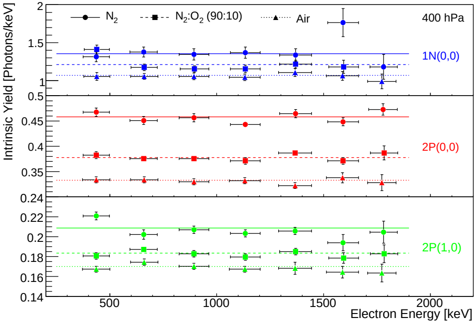

Energy deposit profiles

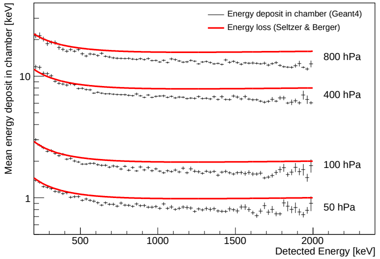

$\Rightarrow$ No energy dependence of $Y^0_{v'}(E)$ in investigated range. $\Leftrightarrow$ $N_\gamma \propto E_{dep}$

Intrinsic Yields of dry air in [Photons/keV]

	2P(0,0)	2P(1,0)	1N(0,0)
This work	$0.338 \pm 0.001 \pm 0.051$	$0.172 \pm 0.001 \pm 0.025$	$1.048 \pm 0.007 \pm 0.154$
Nagano et al.	$0.272 \pm 0.007 \pm 0.035$	$0.122 \pm 0.007 \pm 0.016$	$0.303 \pm 0.012 \pm 0.039$

Step 2: Energy dependence of Intrinsic Yield

Determination of intrinsic yield in sub-samples of 250 keV energy bins:

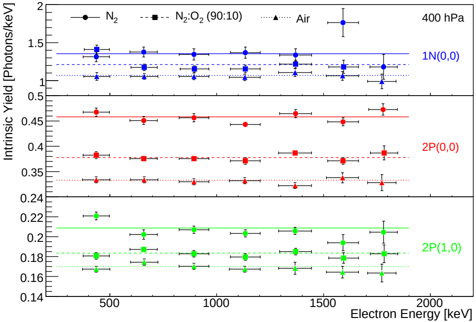

Fluorescence Yield:

$$Y^0_{v'}(E) \cdot R_{v',v''} \cdot \frac{\tau_{v'}(p,T)}{\tau_{0\,v'}} = \frac{N_\gamma(E,p,T)}{N_e \cdot \langle E_{dep}(E,p,T)\rangle}$$

- $R_{v',v''}$, $\tau_{v'}(p,T)$ and $\tau_{0\,v'}$ known from Step 1.
- Deposited energy $\langle E_{dep}(E,p,T)\rangle$ determined by GEANT4 simulation.
- Number of emitted photons $N_\gamma(E,p,T)$ obtained from fit.

$\Rightarrow$ No energy dependence of $Y^0_{v'}(E)$ in investigated range. $\Leftrightarrow$ $N_\gamma \propto E_{dep}$

Intrinsic Yields of dry air in [Photons/keV]

	2P(0,0)	2P(1,0)	1N(0,0)
This work	$0.338 \pm 0.001 \pm 0.051$	$0.172 \pm 0.001 \pm 0.025$	$1.048 \pm 0.007 \pm 0.154$
Nagano et al.	$0.272 \pm 0.007 \pm 0.035$	$0.122 \pm 0.007 \pm 0.016$	$0.303 \pm 0.012 \pm 0.039$

Fluorescence Spectrum at Shower Maximum

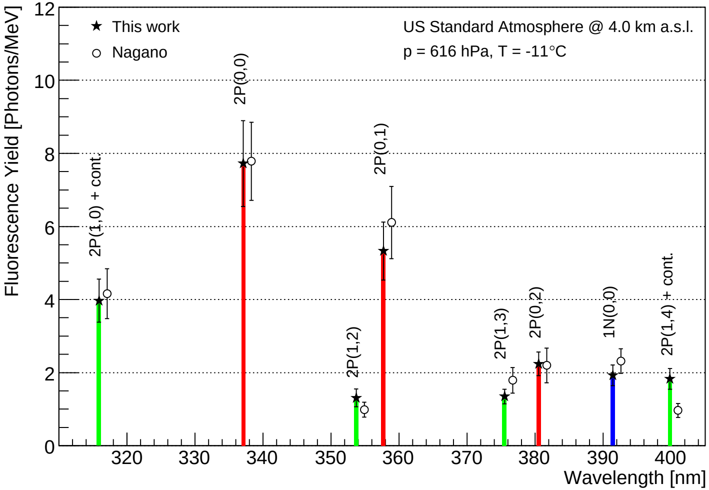

- Good overall agreement with Nagano et al. at this particular height.
- 2P(1,0) and 2P(1,4) bands still contaminated by other transitions.

Fluorescence Yield vs. Height in dry Air

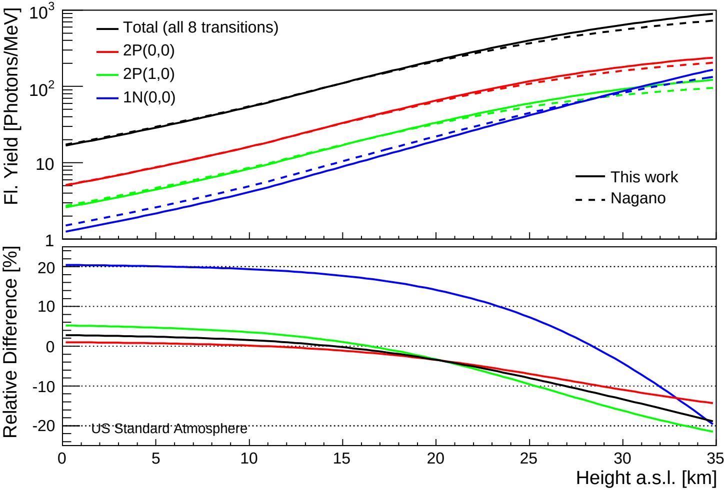

- Below 10 km total yield of Nagano about 3 % larger than this works values.
- Large differences for 1N(0,0) transition.

The Effect of Water Vapor

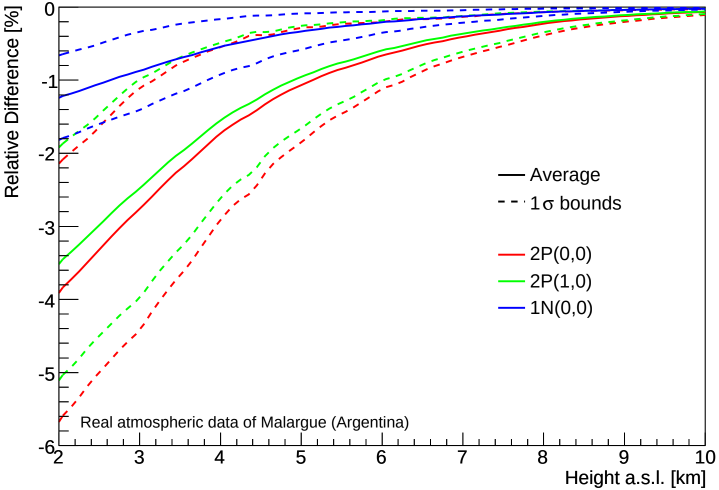

- Average yield reductions at Auger site up to 4 %.
- Differences to Nagano up to 7 % if water vapor quenching is taken into account.

Summary

Achieved so far:

- Nitrogen fluorescence spectrum is superposition of individual sub-spectra.
- Transitions of each sub-spectrum underlie several physical relations.
- The data of the AirLight-Experiment was analyzed according to these relations.
- Global analysis results in consistent description of the fluorescence yield with a minimal set of parameters.
- Fluorescence yield does not depend on energy in investigated range.
- Absolute uncertainties of single nitrogen bands $\lesssim 15$ %.
- Water vapor additionally reduced the fluorescence yield up to 4 %.

Ongoing work:

- Reduction of absolute uncertainties to $\lesssim 10$ % by end-to-end calibration using Rayleigh-Scattering of a 337 nm N_2-laser beam.

Ph.D. Thesis in english: http://bibliothek.fzk.de/zb/berichte/FZKA7209.pdf (paper coming soon)